ORCA – Online Research @ Cardiff

Tris-heteroleptic iridium complexes based on cyclometalated ligands with different cores

Yanouk Cudré,[a] Felipe Franco de Carvalho,[b] Gregory R. Burgess,[a] Louise Male,[a] Simon J. A. Pope,[c] Ivano Tavernelli,[d] Etienne Baranoff[a]*

[a] School of Chemistry, University of Birmingham, Edgbaston, B15 2TT Birmingham, UK. E-mail: EB.Chimie@gmail.com

[b] École Polytechnique Fédérale de Lausanne, CH-1015 Lausanne, Switzerland

[c] School of Chemistry, Main Building, Cardiff University, Park Place, Cardiff, Wales CF10 3AT UK

[d] IBM Research GmbH, Zurich Research Laboratory, 8803 Rüschlikon, Switzerland

Abstract. A series of tris-heteroleptic iridium complexes of the form [Ir(C^N^1)(C^N^2)(acac)] combining 2-phenylpyridine (ppy), 2-(2,4-difluorophenyl)pyridine (dFppy), 1-phenylpyrazole (ppz) and 1-(2,4-difluorophenyl)pyrazole (dFppz) as the C^N ligands has been synthesized and fully characterized by NMR, X-ray crystallography, UV−vis absorption and emission spectroscopy, and electrochemical methods. It is shown that "static properties" (e.g. absorption and emission spectra and redox potentials) are primarily dictated by the overall architecture of the complex, while "dynamic properties" (e.g. excited state lifetime, radiative and nonradiative rate constants) are, in addition, sensitive to the specific positioning of the substituents. As a result, the two complexes

[Ir(dFppy)(ppz)(acac)} and [Ir(ppy)(dFppz)(acac)] have same emission maxima and redox potentials but their radiative and nonradiative rate constants differ significantly by a factor ~2. Then acac (acetylacetonate) was replaced by pic (picolinate) and two pairs of diastereoisomers were obtained. As expected the use of pic as ancillary ligand results in blue-shifted emission, stabilisation of the oxidation potential and improvement of the photoluminescence quantum yield and only minor differences in optoelectronic properties are found between the two diastereoisomers of each pair.

Introduction.

Cyclometalated iridium complexes are widely studied for a range of applications including solar energy conversion,[1-8] organic light emitting diodes (OLEDs),[9-25] light-emitting electrochemical cells (LEECs),[26-34] sensing,[35-39] imaging,[40-43] and synthetic methodologies.[44,45] For more than two decades, these complexes have been particularly appealing because of the excellent performance of their excited states, specifically their relatively short triplet excited state lifetimes, wide colour tunability, and generally high phosphorescence quantum yield.[46-49]

The photophysical and electrochemical properties of the complexes are crucial for the performance of the materials for a given application and different applications may require a different set of properties. Interestingly, these properties can be precisely adjusted through engineering of the chemical structure of the complexes. However, because these properties are ultimately all linked to the same chemical structure, modifications to tune a given attribute also cause undesired variations in many others. For example, the most common strategy to blue-shift the emission of cyclometalated iridium complexes is to introduce electron-withdrawing substituents, in particular fluorine, on the orthometalated phenyl group. By stabilizing the HOMO (highest occupied molecular orbital) more than the LUMO (lowest unoccupied molecular orbital), an increased HOMO-LUMO gap is obtained, which generally translates into emission at higher energy. However, stabilizing the HOMO also means an increase of the oxidation potential. As such the complex *fac*-[Ir(ppy)$_3$] (ppy: 2-

phenylpyridine) emits at 510 nm in dichloromethane at room temperature and has an oxidation potential E_{ox} = 0.31 V *vs* Fc^+/Fc, while the complex *fac*-[Ir(dFppy)$_3$] (dFppy: 2-(2,4-difluorophenyl)pyridine) emits at 468 nm and has E_{ox} = 0.78 V *vs* Fc^+/Fc.[50] It is only recently that the rationalisation of the effect of substituents on HOMO and LUMO energies allows for tuning the emission colour independently of the energy of the HOMO using electron-donating groups.[51]

The radiative and non-radiative rate constants, respectively k_r and k_{nr}, make for another set of parameters crucial to the performance of the emissive complexes as they dictate the photoluminescence quantum yield (PLQY, Φ) and lifetime of excited state (τ). Across a series of complexes, k_r is generally rationalised based on the amount of metal character in the emitting excited state and the energy gap between the singlet and triplet states, while k_{nr} is explained with intramolecular vibronic coupling and thermal accessibility of metal-centred states.[52-56] A number of design strategies have been used to control the rate constants to improve the properties of the emitting state. A major drawback of these strategies is that they invariably result in concomitant variation of the emission colour and/or redox potentials of the complexes because of the intimate interplay between chemical structure and properties.[57-59] Therefore distinguishing the exact effect of a structural modification on specific properties is still a major challenge.

Herein, a design approach allowing variation of the radiative and non-radiative rate constants independently of the emission maximum and redox potential is demonstrated. Our strategy is based on tris-heteroleptic complexes using cyclometalated ligands (C^N) having different cores. Compared to tris-homoleptic [Ir(C^N)$_3$] and bis-heteroleptic [Ir(C^N)$_2$(*La*)] (*La*: ancillary ligand) complexes, tris-heteroleptic complexes [Ir(C^N^1)(C^N^2)(C^N^3 or *La*)] form a new family of complexes attracting increased attention.[60-70] Although often challenging to synthesise and purify, they offer unparalleled opportunities for the fine-tuning of properties. However, up to date, only C^N ligand with same chemical core but different substitution pattern have been used to prepare tris-heteroleptic complexes. Phenyltriazole with adamantyl and methyl substituents and phenylpyridine with, for example, fluorine, methyl, benzo, carbonyl substituents have been reported.
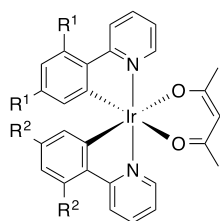
1 $R^1 = R^2 = H$: Ir(ppy)$_2$(acac)
2 $R^1 = R^2 = F$: Ir(dFppy)$_2$(acac)
3 $R^1 = F, R^2 = H$: Ir(dFppy)(ppy)(acac)
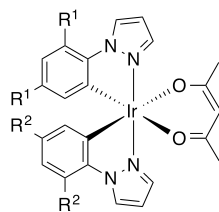
4 $R^1 = R^2 = H$: Ir(ppz)$_2$(acac)
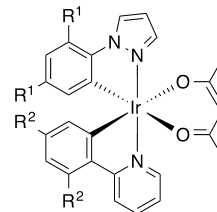**5** $R^1 = R^2 = F$: Ir(dFppz)$_2$(acac)
6 $R^1 = F, R^2 = H$: Ir(dFppz)(ppz)(acac)

7 $R^1 = R^2 = H$: Ir(ppz)(ppy)(acac)
8 $R^1 = R^2 = F$: Ir(dFppz)(dFppy)(acac)
9 $R^1 = H, R^2 = F$: Ir(dFppy)(ppz)(acac)
10 $R^1 = F, R^2 = H$: Ir(dFppz)(ppy)(acac)
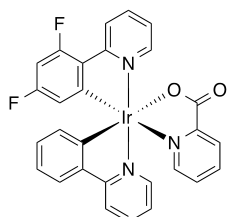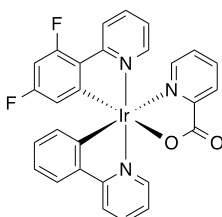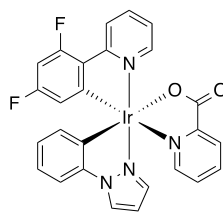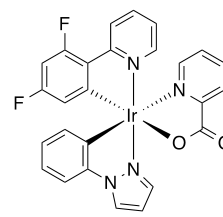
3a   **3b**   **9a**   **9b**

Scheme 1. Chemical structures of the complexes studied. Only the Λ isomers are shown, while all complexes have been isolated as mixture of Δ and Λ isomers.

We have prepared a series of [Ir(C^N^1)(C^N^2)(acac)] complexes (acac: acetylacetonate) with C^N^1 and C^N^2 being ppy, dFppy, ppz (1-phenylpyrazole) and dFppz (1-(2,4-difluorophenyl)pyrazole) making 6 tris-heteroleptic and 4 bis-heteroleptic complexes (Scheme 1). Note the abbreviation for the specific ligand and the full name for the core family of ligand (*e.g.* "ppy" specifically represents the non substituted 2-phenylpyridine ligand, while "phenylpyridine" represents any 2-phenylpyridine ligand with or without substituents).

Firstly, different experimental conditions have been tested to evaluate the possibility of improving the yields of reactions. Then all complexes have been isolated and characterized and their electrochemical and photophysical properties measured. The complexes **1-3** with both phenylpyridine-based ligands have been previously reported. As expected, the complexes **4-6** with both phenylpyrazole-based main ligands are not emissive at room temperature. The complexes **7-10** with mixed phenylpyridine/phenylpyrazole main ligands display emission properties most similar to the phenylpyridine ligand used, ppy or dFppy. As such the phenylpyrazole ligand acts as an ancillary ligand perturbing the excited state on the phenylpyridine ligand. As a result, for complexes containing at least one chromophoric phenylpyridine ligand, the redox potentials and emission maxima are dictated by the overall number of fluorine substituents on the complexes, while k_r and k_{nr}, hence Φ and τ, are dictated

by the presence or absence of pyrazole and, for complexes with only two fluorine atoms, their position on either phenylpyridine or phenylpyrazole. In a second part, the acac of complexes **3** and **9** is replaced with pic (picolinate). Contrary to acac, pic is an asymmetric ligand and two diastereoisomers are obtained for each complex with one having the pyridine of pic *trans* to the phenyl of dFppy and one having the oxygen of pic *trans* to dFppy, Scheme 1. Isolating these diastereoisomers, we show that the properties of two diastereoisomers are very similar, which is confirmed by theoretical calculations. Furthermore, theoretical calculations show that the increased efficiency of non-radiative deactivation processes with phenylpyrazole is mainly due to changes in vibronic coupling, not to thermally accessible metal centred states.

Results and discussion

Synthesis

All tris-heteroleptic acac complexes **3** and **6-10** were synthesized in two steps starting with heating the selected ligands in the presence of an iridium source, $IrCl_3.xH_2O$ or $[Ir(COD)Cl]_2$ (COD: cyclooctadiene), to obtain a mixture of chloro-bridged dimers, followed by reaction with sodium acetylacetonate (acacNa) in CH_2Cl_2/MeOH solvent mixture overnight. This results in a mixture of complexes containing the target tris-heteroleptic acac complex with the two corresponding bis-heteroleptic complexes, $[Ir(ppy)_2(acac)]$ **1**, $[Ir(dFppy)_2(acac)]$ **2**, $[Ir(ppz)_2(acac)]$ **4** or $[Ir(dFppz)_2(acac)]$ **5**.

As the relative amount of the target tris-heteroleptic complex compared to bis-heteroleptic complexes is embedded in the mixture of chloro-bridged iridium dimers, different reaction conditions for the first step have been explored as a possible means to improve the yield of tris-heteroleptic complexes. Three sets of conditions were tested: (Cond. A) $IrCl_3.xH_2O$ as iridium source with ethoxyethanol/water as solvent, heating at 130 °C for 12 hours; (Cond. B) $[Ir(COD)Cl]_2$ as iridium source with ethoxyethanol as solvent, heating at 130 °C for 3 hours; (Cond. C) $[Ir(COD)Cl]_2$ as iridium source with xylene as solvent, heating at 130 °C for 3 hours. Conditions A are the most commonly used conditions for the synthesis of chloro-bridged iridium dimers. Conditions B have been previously used for the synthesis of the tris-heteroleptic complex **1** where the use of an Ir(I) starting material tremendously decreased the reaction time from 12h to 3h.[60] Condition C was chosen to briefly explore the effect of the solvent and are slightly modified from a previously reported methodology.[71]

5

Because the reaction of the iridium chloro-bridged dimers with acacNa is quasi quantitative in the conditions used, the ^{1}H NMR analysis of the mixture resulting from such reaction is a reasonable proxy for the composition of the mixture of dimers. The direct analysis of the mixture of dimers would have been an unnecessarily tedious task due to their poor solubility in most solvents and because of the high number of species generated by the reaction (seven dimers are possible). As expected, the ^{1}H NMR signals from the crude are a perfect combination of the signals from the purified products (Figure S1-S6), which gives access to the relative amount of each complex from the integration of the signals. An average molar mass was calculated from the ratio obtained, which rapidly gives access to an approximate yield for each complex without the need for purification. Isolated yields of target complexes were judged less appropriate for this discussion due to the possible partial degradation of the complexes on acidic silica during purification.[60]

Table 1. ^{1}H NMR yields of reactions

Entry	C^N1	C^N2	Cond.[a]	Yield % [Ir(C^N1)$_2$(acac)]		Yield % [Ir(C^N2)$_2$(acac)]		Yield % [Ir(C^N1)(C^N2)(acac)]		Overall yield %
1	ppy	dFppy	A	**1**	18	**2**	19	**3**	30	67
2			B		12		12		38	62
3			C		16		15		42	73
4	ppy	ppz	A	**1**	13	**4**	30	**7**	14	57
5			B		23		4		43	70
6			C		11		2		32	45
7	ppy	dFppz	A	**1**	9	**5**	22	**10**	28	59
8			B		19		3		16	38
9			C		15		7		19	41
10	dFppy	ppz	A	**2**	22	**4**	19	**9**	30	71
11			B		33		4		18	55
12			C		17		2		36	55
13	dFppy	dFppz	A	**2**	25	**5**	14	**8**	29	68
14			B		24		5		32	61
15			C		24		5		24	53
16	ppz	dFppz	A	**4**	22	**5**	10	**6**	36	68
17			B		4		6		14	24
18			C		4		11		20	35

a) Cond. A: IrCl$_3$, xH$_2$O ethoxyethanol/water, 130 °C, 12 hours; Cond. B :[Ir(COD)Cl]$_2$, ethoxyethanol, 130 °C, 3 hours; Cond. C: [Ir(COD)Cl]$_2$, xylene, 130 °C, 3 hours

The results summarized in Table 1 allow for a qualitative discussion of the reactivity of the ligands. Both in terms of overall yields and yields of tris-heteroleptic complexes, it appears

that condition A was the most generally applicable. Importantly, the tris-heteroleptic complex is the major species, but for entry 4, 8 and 11 of Table 1. Assuming a stepwise coordination of the two ligands to form the final dimer, a two step mechanism can be hypothesised as follows: in step 1, the iridium starting material, "IrCl", reacts with a first ligand to give an intermediate "Ir(C^N)Cl" species that reacts with another ligand in step 2 to give the chloro-bridged dimer. Under condition A using an iridium(III) starting material, both steps can be considered to proceed through electrophilic substitution, while with conditions B and C using an iridium(I) starting material, the first step is ascribed to an oxidative addition followed by an electrophilic substitution. The yield of bis-phenylpyrazole complexes is always low with conditions B and C (entries 5, 6, 8, 9, 11, 12, 14-18), suggesting phenylpyrazole is disfavoured during the oxidative addition. However, this is balanced by the higher reaction rate of the fluorinated ligands.[72] On the other hand, in the case of electrophilic substitution, the reaction rate is disfavoured by the presence of electron-withdrawing groups on the ligand,[72] while the resulting "Ir(C^N)Cl" intermediate complex would be more reactive because of the decreased electron density on the metal. These antagonistic effects explain the absence of clear and meaningful trends and results will depend largely on the type of core ligands and substituents as well as combination of ligands used. In conclusion, using an iridium(I) starting material for the synthesis of heteroleptic dimers leads to the best results in several cases (entries 2, 3, 5, 6, 12, 14), but the use of iridium(III) is more likely to give reasonable to high yield of tris-heteroleptic complexes (only entry 4 shows a low yield).

The acac complexes can be purified using standard chromatography techniques with silica gel (see Figure S7 for TLC analyses), using triethylamine to limit the degradation induced by the acidic silica. The pic complexes were obtained by reacting **3** and **9** with BF_3 in acetonitrile to give the bis-acetonitrile complexes, followed by reaction with picolinic acid in the presence of a base. The diastereoisomers have been purified by HPLC. All isolated complexes have been characterized by NMR (^{1}H, ^{13}C, ^{19}F, COESY, NOESY, HMQC), HRMS, FT-IR spectroscopy, and their purity evaluated with analytical HPLC and elemental analysis (Figures S8-S17).

Complex 3a   Complex 3b   Complex 9a   Complex 9b
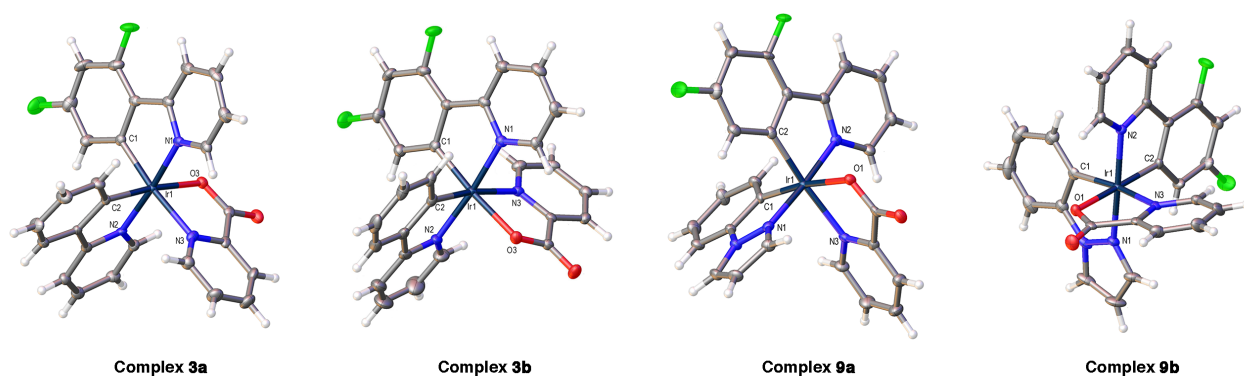
Figure 1. X-ray crystal structures of **3a**, **3b**, **9a** and **9b** with ellipsoids drawn at the 50% probability level.

X-ray crystal structures.

X-ray crystal structures were obtained for all new tris-heteroleptic complexes and they confirm the chemical structure of the isomers **3a-b** and **9a-b**. Single crystals have been grown by slow diffusion of hexane into a dichloromethane solution of the complexes. The structures of **3a**, **3b**, **9a** and **9b** are shown in Figure 1 and selected crystallographic data are provided in Table 2 and Table 3. Details for all others structures are given in the supporting information.

Table 2. Comparison between experimental and theoretical ground state geometries for **3a-b** and **9a-b**

bond lengths [Å]								
	3a		**3b**		**9a**		**9b**	
	DFT	X-ray	DFT	X-ray	DFT	X-ray	DFT	X-ray
Ir-N$_{pic}$	2.16	2.132(4)	2.16	2.124	2.16	2.136	2.15	2.120
Ir-N$_{C^N}$	2.05	2.037(4)	2.05	2.036	2.03	2.026	2.03	2.028
Ir-N$_{dFppy}$	2.00	2.034(4)	2.04	2.033	2.04	2.034	2.04	2.032
Ir-O$_{pic}$	2.18	2.162(3)	2.04	2.152	2.17	2.150	2.18	2.158
Ir-C$_{C^N}$	2.00	1.990(3)	2.01	2.006	2.01	2.008	2.03	2.010
Ir-C$_{dFppy}$	2.00	2.001(4)	1.99	1.987	2.00	1.980	1.99	1.996
angles [º]								
	3a		**3b**		**9a**		**9b**	
	DFT	X-ray	DFT	X-ray	DFT	X-ray	DFT	X-ray
C$_{dFppy}$-Ir-C$_{C^N}$	89.53	89.6(3)	89.56	89.760	89.09	88.736	89.33	95.137
N$_{dFppy}$-Ir-N$_{C^N}$	175.28	175.67(15)	175.20	174.697	174.71	175.923	174.75	174.081
C$_{C^N}$-Ir-N$_{C^N}$	80.52	80.942	80.27	80.521	79.86	80.889	79.49	80.282
C$_{dFppy}$-Ir-N$_{C^N}$	95.52	95.321	97.09	95.036	95.50	96.446	96.84	95.212
C$_{dFppy}$-Ir-N$_{dFppy}$	80.35	80.746	80.62	81.020	80.44	80.694	80.71	80.934
C$_{dFppy}$-Ir-O$_{pic}$	96.85	95.103	173.99	174.675	96.77	96.817	173.24	175.764

Table 3. Crystallographic data for **3a-b** and **9a-b**[a]

	3a	3b•3/2 CH$_2$Cl$_2$,0.5 H$_2$O	9a	9b•3/2 CH$_2$Cl$_2$
CCDC number	1552222	1552223	1511802	1511803
Empirical formula	C$_{28}$H$_{18}$F$_2$IrN$_3$O$_2$	C$_{29.5}$H$_{22}$Cl$_3$F$_2$IrN$_3$O$_{2.5}$	C$_{26}$H$_{17}$F$_2$IrN$_4$O$_2$	C$_{27.5}$H$_{20}$Cl$_3$F$_2$IrN$_4$O$_2$
Formula weight (g/mol)	658.65	795.05	647.63	775.02
Temperature (K)	100.01(10)	100.01(10)	99.97(10)	100.01(10)
Crystal system	orthorhombic	monoclinic	monoclinic	monoclinic
Space group	Pna2$_1$	P2$_1$/c	P2$_1$/n	P2$_1$/c
a (Å)	15.0856(2)	16.7317(5)	9.2743(3)	16.3715(4)
b (Å)	16.3361(2)	12.3412(2)	14.7104(4)	12.2266(2)
c (Å)	9.47782(13)	15.5940(4)	16.5135(5)	15.6859(4)
α (°)	90	90	90	90
β (°)	90	117.541(4)	93.301(3)	118.521(3)
γ (°)	90	90	90	90
Volume (Å^3)	2335.71(6)	2855.09(15)	2249.18(11)	2758.76(13)
Z	4	4	4	4
ρ$_{calc}$ (g/cm^3)	1.873	1.850	1.913	1.866
μ (mm^{-1})	5.764	5.006	11.923	12.455
F(000)	1272.0	1544.0	1248.0	1500.0
Crystal size (mm^3)	0.1932 × 0.1488 × 0.1233	0.2164 × 0.1215 × 0.0362	0.2106 × 0.0601 × 0.0459	0.4159 × 0.1754 × 0.0943
θ range for data collection (°)	4.968 to 54.958	5.892 to 50.688	8.056 to 136.498	6.144 to 144.228
Reflections collected	24233	14404	12463	16925
Independent reflections	5197 [R$_{int}$ = 0.0312, R$_{sigma}$ = 0.0267]	5204 [R$_{int}$ = 0.0269, R$_{sigma}$ = 0.0321]	4103 [R$_{int}$ = 0.0353, R$_{sigma}$ = 0.0347]	5406 [R$_{int}$ = 0.0310, R$_{sigma}$ = 0.0253]
Data/restraints/parameters	5197/1/325	5204/0/415	4103/0/316	5406/0/397
Goodness-of-fit on F^2	1.057	1.025	1.105	1.078
Final R indexes [I>=2σ (I)]	R$_1$ = 0.0178, wR$_2$ = 0.0348	R$_1$ = 0.0258, wR$_2$ = 0.0606	R$_1$ = 0.0314, wR$_2$ = 0.0803	R$_1$ = 0.0350, wR$_2$ = 0.0841
Final R indexes (all data)	R$_1$ = 0.0214, wR$_2$ = 0.0364	R$_1$ = 0.0314, wR$_2$ = 0.0637	R$_1$ = 0.0361, wR$_2$ = 0.0840	R$_1$ = 0.0356, wR$_2$ = 0.0845

As expected, all complexes have a slightly deformed octahedral coordination geometry around the iridium center with the usual cis-C,C trans-N,N chelate configuration.

Table 4. Photophysical and photochemical properties of complexes **1-10, 3a-b** and **9a-b**.

	E$_{ox}$ (V)[d]	E$_{red}$ (V)[d]	λ$_{abs}$ (nm), (ε 10^3 L mol^{-1} cm^{-1})[a]	λ$_{em}$ (nm), RT[b]	τ (ns), RT[b]	Φ$_{PL}$[b]	k$_r$ (10^5 s^{-1})	k$_{nr}$ (10^5 s^{-1})
1	0.43 (0.41)[c]	−2.57 (−2.60)[c]	260 (39.15), 340 (9.15), 405 (4.02), 459 (2.88), 489 (1.32)	519 (520)[c]	1511 (1227)[c]	0.47[c]	3.83[c]	4.32[c]
2	0.73 (0.76)[c]	−2.45 (−2.44)[c]	253 (45.72), 328 (11.44), 389 (4.72), 435 (2.23), 466 (0.82)	482 (484)[c]	898 (872)[c]	0.63[c]	7.22[c]	4.24[c]
3	0.58	−2.51	256 (42.97), 334 (10.34), 398	503	1413	0.69[c]	5.64[c]	2.53[c]

	(0.57)[c]	(−2.52)[c]	(4.29), 449 (2.44), 479 (0.79)	(503)[c]	(1224)[c]			
4	0.49	–	252 (34.04), 297 (15.15), 330 (8.57), 377 (2.77), 418 (0.19)	–	–	–	–	–
5	0.79	–	253 (31.19), 321 (8.06), 359 (2.23), 400 (0.29)	–	–	–	–	–
6	0.64	–	251 (33.18), 269 (25.53), 294 (13.89), 325 (8.61), 370 (2.21), 408 (0.15)	–	–	–	–	–
7	0.45	−2.58	256 (36.36), 295 (17.76), 335 (8.81), 374 (4.14), 405 (2.35), 456 (1.27), 487 (0.38)	519	1592	0.26	1.63	4.65
8	0.75	−2.44	253 (40.40), 289 (18.86), 325 (10.349), 361 (3.95), 385 (2.52), 430 (0.95), 461 (0.31)	483	619	0.22	3.55	12.60
9	0.61	−2.50	254 (35.00), 291 (16.91), 330 (8.85), 369 (3.63), 392 (2.21), 437 (1.01), 469 (0.37)	503	837	0.32	3.82	8.12
10	0.60	−2.52	257 (35.63), 295 (17.39), 328 (9.17), 360 (4.28), 396 (2.36), 430 (1.46), 478 (0.32)	502	1575	0.30	1.90	4.44
3a	0.73	−2.33	261 (37.55), 289 (20.99), 323 (10.15), 345 (5.81), 390 (3.87), 431 (2.33), 462 (0.27)	489	1850	0.49	2.65	2.76
3b	0.72	−2.34	259 (32.69), 289 (18.54), 305 (13.67), 322 (9.37), 345 (5.39), 389 (3.66), 430 (2.14), 470 (0.23)	485	1559	0.43	2.76	3.66
9a	0.76	−2.35	253 (36.20), 283 (20.92), 303 (14.62), 321 (10.91), 341 (6.86), 383 (3.28), 415 (1.65), 432 (0.93), 460 (0.24)	499	1004	0.42	4.18	5.78
9b	0.73	−2.33	258 (31.18), 281 (16.35), 302 (12.57), 322 (7.66), 341 (4.18), 384 (2.34), 414 (1.42), 431 (0.84), 458 (0.19)	498	971	0.38	3.91	6.39

[a]aerated dichloromethane. [b]degassed dichloromethane. [c]according to ref. 60. [d]degassed acetonitrile/TBAPF$_6$ 0.1M, vs Fc$^+$/Fc at 1V/s.
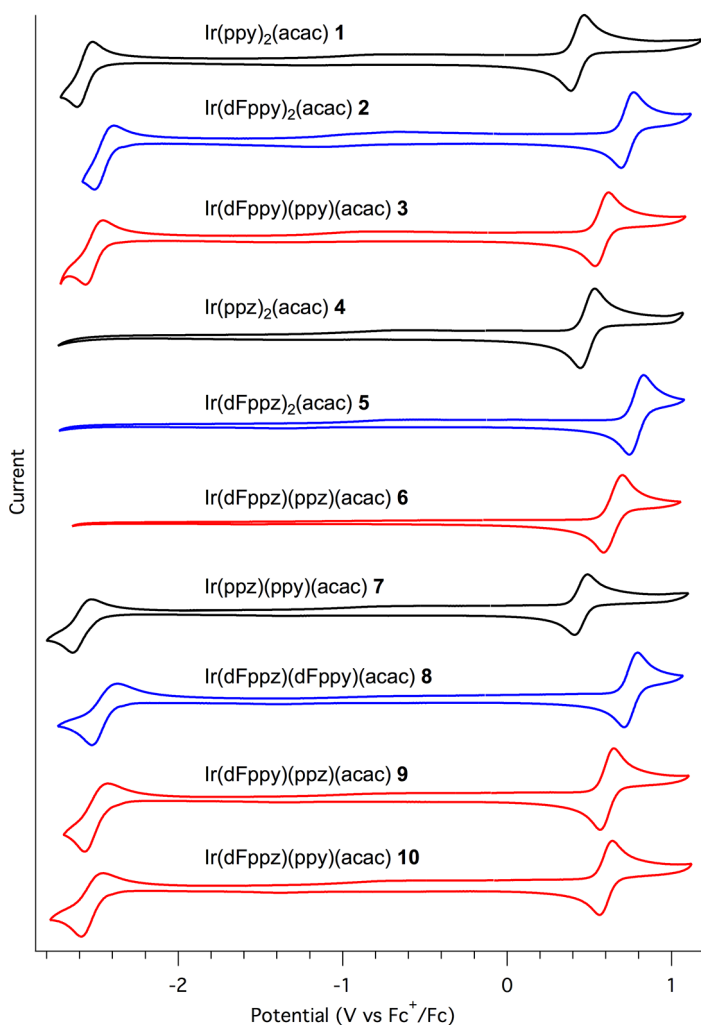
Figure 2. Cyclic volamograms of complexes **1-10**. (—) Complexes with no fluorine atoms; (—) Complexes with 4 fluorine atoms; (—) Complexes with 2 fluorine atoms.

Electrochemistry

The oxidation and reduction potentials were measured by cyclic voltammetry in degassed acetonitrile containing 0.1 M tetrabutyl ammonium hexafluorophosphate (TBAPF$_6$). The data are summarized in Table 4; the voltammograms are shown in Figure 2 for the acac complexes and in Figure 3 for the pic complexes.

All pyridine-containing complexes show quasi-reversible oxidation and reduction potentials. As expected, the reduction potentials of the bis-pyrazole complexes **4**, **5** and **6** are outside the limit of the system and are therefore not measurable. As the oxidation potentials correspond to the oxidation of the iridium center, the values are primarily controlled by the overall number of fluorine substituents on the complexes with a minor effect of the presence of pyrazole, about 30 mV per pyrazole unit replacing a pyridine unit. As such, complexes

without fluorine have E_{ox} ranging from +0.42 to +0.49 *vs* Fc⁺/Fc, while addition of two fluorine substituents shifts the range to +0.58 to +0.64 *vs* Fc⁺/Fc and four fluorine shifts the range further to +0.74 to +0.79 *vs* Fc⁺/Fc. The effect of fluorine substituents can also be seen on the reduction potentials (no fluorine: −2.57 to −2.58; two fluorine: −2.50 to −2.52 and four fluorine: −2.44 to −2.45 *vs* Fc⁺/Fc) with virtually no effect of replacing a pyridine with a pyrazole due to the reduction being localized on the phenylpyridine ligand.

For complexes **9**, [Ir(dFppy)(ppz)(acac)], and **10**, [Ir(ppy)(dFppz)(acac)], the data are particularly interesting as they show comparable values for the oxidation and reduction potentials. This suggests that the effect of the 2,4-difluorination of the phenyl ring is independent of the ligand being fluorinated. In contrast, the radiative and non-radiative rate constants are largely influenced by the position of the 2,4-difluorination (see below). In addition, these two complexes display very similar redox potentials to those of complex **3**, [Ir(dFppy)(ppy)(acac)], besides a small 20 mV shift to lower oxidation potential with **3** due to the absence of the pyrazole unit. This demonstrates that tris-heteroleptic complexes provide the possibility for different complex designs that have the same HOMO and LUMO energies and same emission maxima (see below), while each of these designs can exhibit different values for k_r and k_{nr}
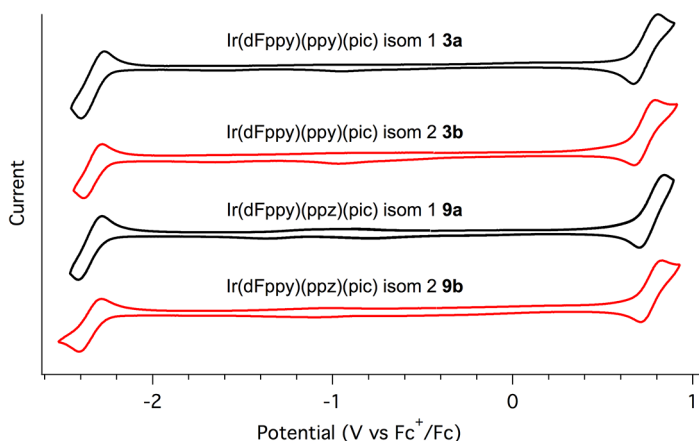
Figure 3. Cyclic volamograms of complexes **3a-b** and **9a-b**. (—) Isomers with N-pic *trans* to dFppy; (—) Isomers with O-pic *trans* to dFppy.

As the two pairs of diastereoisomers **3a-b** and **9a-b** contain at least one pyridine group, they also show quasi-reversible oxidation and reduction potentials (Figure 3). The principal effect of replacing acac with pic is to anodically shift both oxidation and reduction potentials by ~150 mV without changing the electrochemical gap (3.06-3.11 eV compared to 3.09-3.10 for

3 and **9**). The four complexes display very similar redox potentials demonstrating further that these energy levels are primarily dependent on the overall structure and composition of the complexes, and not on the particularities of the chemical structures. This is confirmed by theoretical calculations (see Supporting information) showing that the localization of the HOMOs and LUMOs are similar for the four complexes. Furthermore, the orbitals of these complexes are similar to those of FIrpic, another well studied Ir complex, which is not surprising considering the similarity between these molecules.[73-78] In their ground-state, **3a-b** and **9a-b** isomers all have HOMOs composed of significant Ir(5d) character, at around 50%. All the occupied orbitals have some degree of Ir(5d) character and some ligand π orbital character, with the maximum Ir(5d) contribution appearing in HOMO-1 at 61% for **3a-b**; in HOMO-2 at 67% for **9a**, and in HOMO-1 at 60% for **9b**. The lower lying unoccupied orbitals have much lower Ir(5d) character (at around 1%) and are mostly ligand-centred.
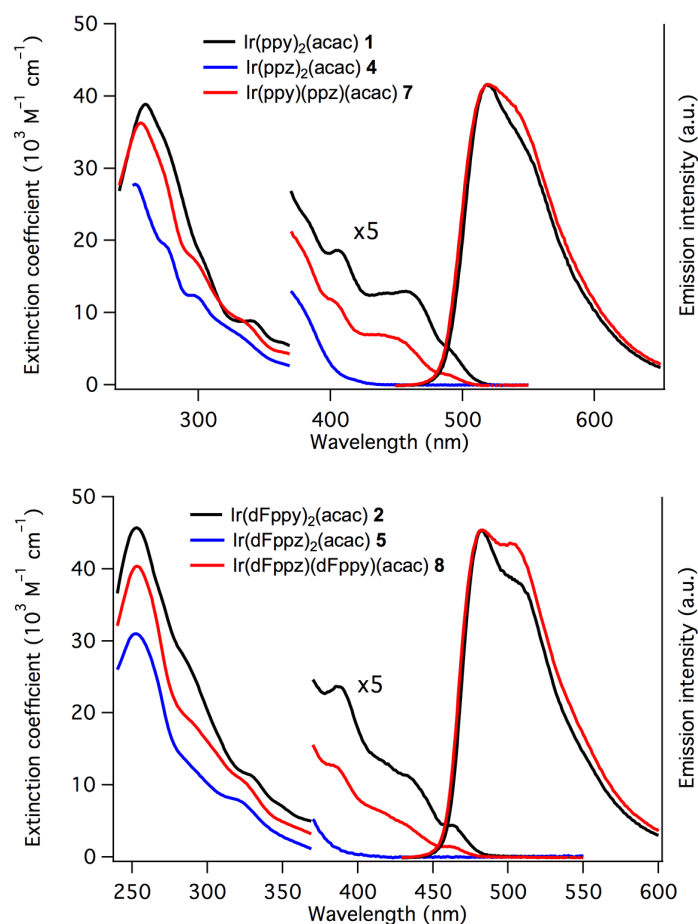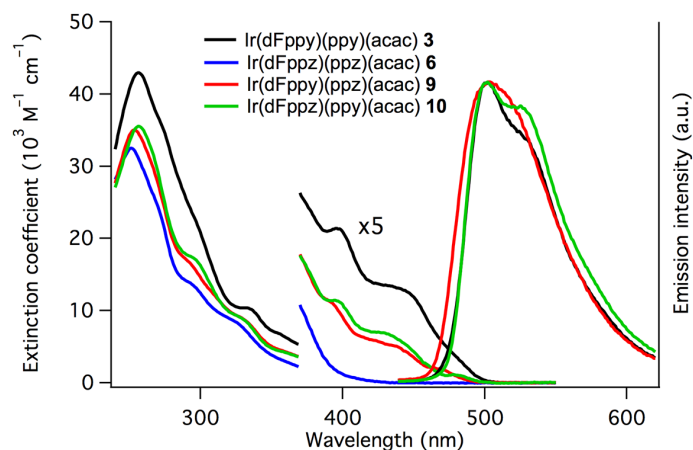
Figure 4. Absorption (left) and emission (right) spectra measured at room temperature in dichloromethane (abs.) and in degassed dichloromethane (em.) of: Top: **1**, **4** and **7**; Middle: **2**, **5** and **8**; Bottom: **3**, **6**, **9** and **10**.
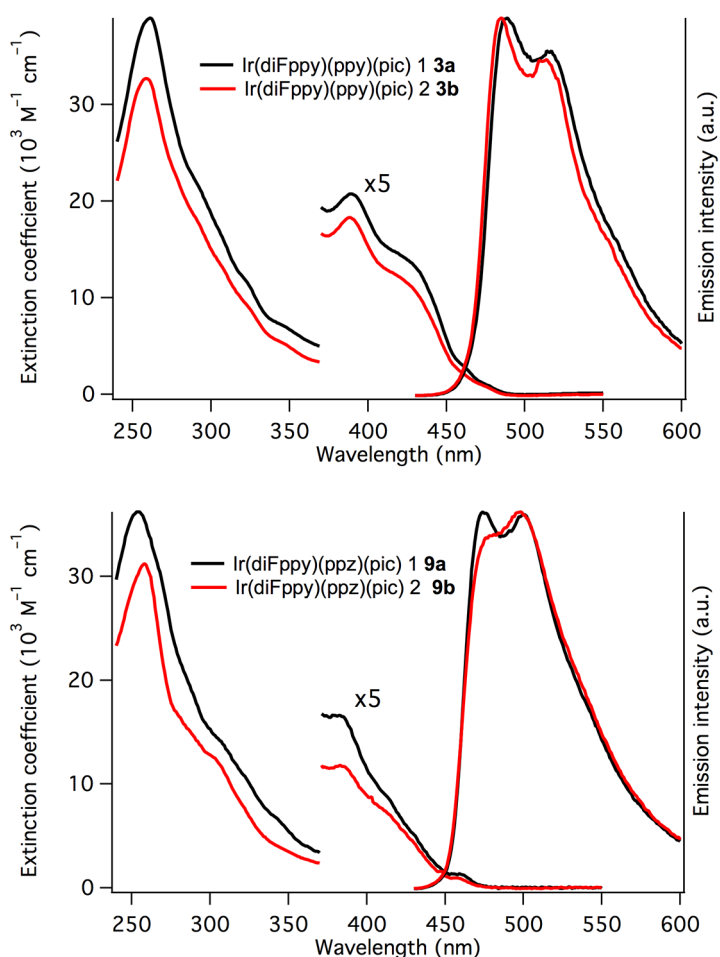
Figure 5. Absorption (left) and emission (right) spectra measured at room temperature in dichloromethane (abs.) and in degassed dichloromethane (em.) of: Top: **3a** and **3b**; Bottom: **9a** and **9b**.

Photophysical properties

The UV-visible electronic absorption spectra and luminescence spectra of complexes **1-10** are shown in Figure 4 and the spectra for complexes **3a-b** and **9a-b** are shown in Figure 5. Data are summarized in Table 4.

As for other cyclometalated iridium complexes, the absorption spectra are dominated by strong absorption bands at 254 to 260 nm ($\varepsilon \sim 30\text{-}45 \times 10^3$ M^{-1} cm^{-1}) attributed to ligand centred (LC) $^1\pi\pi^*$ transitions followed by weaker transitions ($\varepsilon \sim 5\text{-}20 \times 10^3$ M^{-1} cm^{-1}) of charge transfer character (CT) between 300 and 440 nm corresponding to transitions from the iridium centre to the ligand (MLCT). The last weak transitions ($\varepsilon < 10^3$ M^{-1} cm^{-1}) observed at lowest energy are attributed to direct population of the emitting triplet state. As expected, **4**, **5** and **6** show a blue shifted absorption compared to the phenylpyridine complexes with onset absorptions below 430 nm, coherent with non-measurable reduction potentials, suggesting a high energy LUMO. The absorption profiles in the MLCT regions of **7-10** are very similar to those of their corresponding phenylpyridine-based bis-heteroleptic complex **1** or **2** with roughly halved molar extinction coefficients, due to the presence of only one phenylpyridine ligand. The higher energy transitions between 260 and 350 nm exhibit some more phenylpyrazole-like character such as the 297 nm peak of **4** being visible on **7** (Figure 4) or the 294 and 325 nm peaks of **6** also appearing in **9** and **10** (Figure 4).

The bis-pyrazole complexes **4-6** are not emissive at room temperature. At 77 K in frozen THF, they display a broad emission band with emission maxima at 538, 515 and 503 nm for **4**, **6** and **5**, respectively (Figure S32), hence blue-shifted as the number of fluorine increases. Such band has been previously attributed to a metal-ligand to ligand charge transfer (^{3}MLLCT).[79,80] The emission profiles of the tris-heteroleptic complexes follow the trend of typical Ir complexes with phenylpyridine-based ligands with a blue-shifted emission as the overall number of fluorine substituents is increased. Replacing a pyridine with a pyrazole induces only a minor broadening ($\sim$100 cm^{-1}) of the spectra without changing the emission maxima (**1** *vs* **7**; **2** *vs* **8**; **3** *vs* **9** and **10**). This is in line with the HOMO-LUMO gap also not being affected by the structural change, and demonstrates that for these acac complexes the difference between the electrochemical gap and the optical gap is fairly constant and independent of the presence or not of a pyrazole unit. Combined with the UV-vis profiles and redox potentials, these clues strongly suggest that the excited state is localized on the phenylpyridine ligand.

As seen above, replacing a pyridine with a pyrazole in complexes **1-3** has virtually no effect on the redox potentials and emission spectra. However, such structural modification has a significant impact on the radiative and non-radiative rate constants. Excited state lifetimes and quantum yields have been measured, see Table 4, and used to calculate radiative ($k_r = \Phi/\tau$) and non-radiative ($k_{nr} = (1-\Phi)/\tau$) rate constants assuming unitary intersystem crossing. Compared to the bis-phenylpyridine complexes **1-3**, the phenylpyridine/phenylpyrazole mixed complexes **7-10** display distinctly lower Φ with τ dictated by the chosen phenylpyridine. As such, **7** and **10** that contain ppy have τ = 1.60 and 1.58 μs, respectively, very close to 1.52 μs of Ir(ppy)$_2$(acac) **1**, while **8** and **9** that contain dFppy have τ = 0.62 and 0.84 μs, respectively, very close to 0.90 μs of Ir(dFppy)$_2$(acac) **2**. Similar τ with lower Φ results in lower (down to about half) k_r and higher (up to three times) k_{nr} for the phenylpyridine/phenylpyrazole mixed complexes compared to the bis-phenylpyridine complexes without changing the emission spectra or the redox potentials. This is particularly striking for complexes **9** and **10** that differ only by the position of the 2,4-difluorination: their optoelectronic properties differ only in their largely different excited state lifetime.

The reduction of k_r and increase of k_{nr} induced by the presence of a phenylpyrazole ligand can be rationalized by invoking a perturbative participation of the non-chromophoric phenylpyrazole ligand to the excited state localized on the phenylpyridine ligand. Indeed, studies of [Ir(ppz)$_3$] and [Ir(dFppz)$_3$] have pointed to these complexes having low k_r on the order of 10^4 s^{-1}, high k_{nr} on the order of 10^{12} s^{-1} and an excited state energy of about 3 eV.

When comparing the **a** and **b** diastereoisomers, no significant differences can be found: **3a** and **9a** are very similar to **3b** and **9b**, respectively. The only statement that can be made without exercising too much speculation is that isomers **a** with the pyridine of the pic trans to the dFppy ligand have a slightly higher (about 10%) absorption coefficient throughout the absorption spectra and that their excited state properties are more favourable due to a slightly lower k_{nr}. This close similarity between the two isomers is confirmed by theoretical calculations.
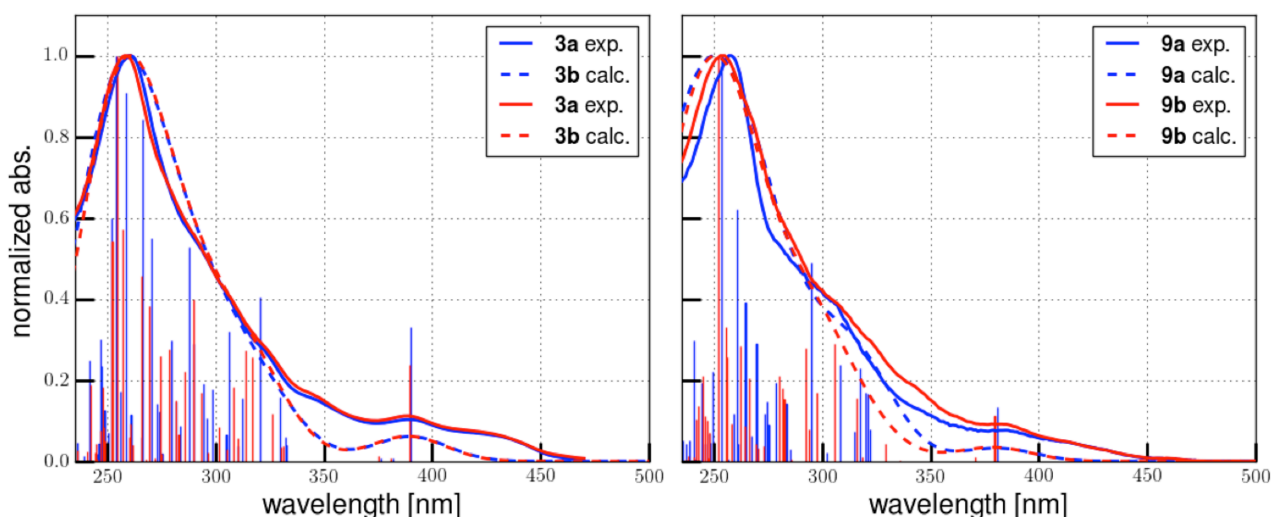
Figure 6. Comparison between experimental and computed absorption spectra. The vertical bars represent the electronic transitions calculated with LR-TDDFT, with their heights being proportional to the oscillator strengths. The dashed lines were obtained by convoluting the experimental results with a Gaussian broadening function of full width at half-maximum of 20 nm.

The absorption spectra at the ground-state equilibrium geometry were calculated using LR-TDDFT. A total of 45 (singlet) states for each complex were computed in order to cover the experimental absorption spectra range. The details of the transitions with largest oscillator strengths are given in Table S10. The spectra obtained with the calculations are in good agreement with experiments (Figure 6). The first excited state (S_1) of both isomers has an MLCT character and a large HOMO→LUMO contribution, which is however less than 50% in all four cases.

The estimates we obtained for the triplet emission peaks – with the U-DFT calculations – were 2.35 eV (527 nm) for **3a**, 2.36 eV (524 nm) for **3b**, 2.49 eV (498 nm) for **9a** and 2.48 eV (500 nm) for **9b**. Experimental peaks are at 2.54 eV (489 nm), 2.56 (485 nm), 2.48 eV (500 nm) and 2.49 eV (498), respectivel. For **3a-b**, our results are slightly redshifted, but well within the expected error of the method.
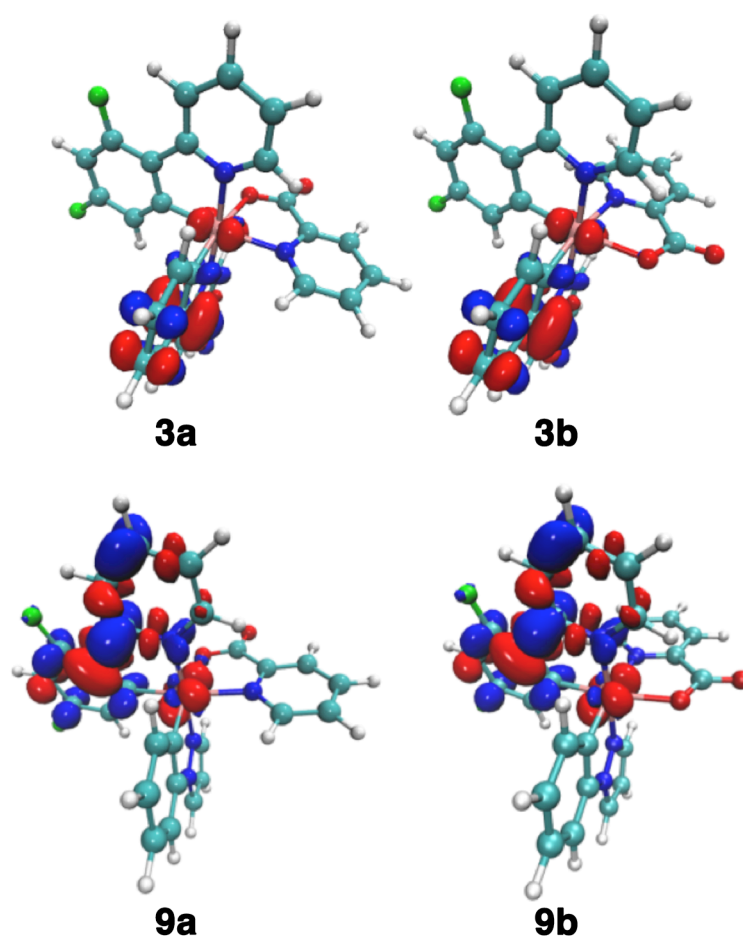
Figure 7. Density differences of **3a-b** and **9a-b** at the LR-TDDFT optimized T_1 geometries. The blue parts represent the positive part of the density (the electron), while the red part represents the negative part (the hole).

The spin-densities calculated at the U-DFT optimized geometries in state T_1 are shown in Figure S41. These transitions have large Ir(5d) contributions and are mostly localized on the ppy ligands for **3a-b** and on the dFppy ligands for **9a-b**, with minor contributions on the pic ligand, and we observe that there is very little difference between the isomers. The same results are obtained with density differences calculated at the LR-TDDFT optimized T_1 geometries (Figure 7). The density differences also show particularly well that the first triplet has a combination of MLCT and LC characters, since we can distinguish the electron (blue color) and hole (red color) contributions to the state. The similarity between the electronic structures – observed in both the spin densities and the density differences – of the two isomers excludes the possibility that it causes difference in broadness observed in the emission spectra. This suggests that this difference is very likely due to vibronic couplings. These vibronic couplings may also be responsible for the nonradiative deactivation of the

excited states.[54,81] Indeed, metal-centred (MC) states are – in all four cases – over 2 eV higher than T_1 (see Supporting Information). Activation energies into the MC state are therefore expected to be also relatively high and thermal activation into these quenching states not very efficient, although only a complete evaluation of the potential energy surfaces upon increasing the metal-ligand bond lengths will accurately answer this question.[82,83] Another deactivation pathway can be due to transitions into poorly emissive metal-ligand (ppy) to ligand (pic) charge transfer states.[82]

Because of the similarities between the isomers, we will briefly discuss the pairs in comparison to their parent acac complexes **3** and **9**. Compared to **3**, **3a-b** show ~0.06 eV blue-shifted absorption and emission spectra, and **9a-b** show ~0.06 eV blue-shifted absorption and ~0.14 eV blue shifted emission spectra compared to **9**. So while both **3** and **9** display emission maxima in the green at 502 nm, **3a-b** emit at 485-489 nm and **9a-b** at 475 nm, both in the bluish-green region with **9a-b** coming close to FIrpic (468 nm) in spite of having only two fluorine substituents.

A change of ancillary ligand is a common strategy to tune the emission color of cyclometalated iridium complexes either because *La* is non-chromophoric and affect the energy of the HOMO much more than the energy of the LUMO[57] or because *La* is chromophoric, which can result in the ancillary ligand being the emitting ligand.[84,85] In our case, pic is a non-chromophoric ligand; therefore changing acac for pic was expected to result in a blue shift due to larger stabilization of the HOMO. As just seen, the emission is indeed blue shifted in complexes **3a-b** and **9a-b** compared to **3** and **9**, respectively. However, this cannot be attributed to a larger stabilization of the HOMO as the electrochemical gap can be considered constant on going from acac to pic (see Electrochemistry section above). Therefore the reasons for the observed blue shift have to be attributed to the additional term differentiating the electrochemical gap with the optical gap.[86]

Conclusion

In summary, a series of tris-heteroleptic cyclometalated iridium(III) complexes Ir(C^N^1)(C^N^2)(acac) (C^N^1, C^N^2: ppy, dFppy, ppz, dFppz) and the corresponding bis-heteroleptic complexes has been synthesized and fully characterized. In addition, the use of picolinate as the ancillary ligand with the [Ir(dFppy)(ppy)] and [Ir(dFppy)(ppz)] cores provided two pairs of diastereoisomers.

Exploration of various reaction conditions to obtain the chloro-bridged iridium dimer showed that both Ir(I) and Ir(III) can be used as starting materials to obtain tris-heteroleptic complexes and that the most suitable depends on the core and substituents of the ligands used.

Photophysical and electrochemical studies showed that absorption, emission wavelength and redox properties are governed primarily by the overall structure of the complexes, while dynamic properties such as radiative and non-radiative constants are controlled by the specific placement of the substituents. As a result, it is possible to vary k_r and k_{nr} without impacting significantly other properties.

When pic was used as the ancillary ligand, it was found that both diastereoisomers have very similar photophysical and electrochemical properties. It may therefore be possible to use the mixture of isomers as materials for application without the need for tedious purification.

Acknowledgements

Supporting Information

Full experimental procedures and characterizations (including NMR spectra, X-ray crystallography, FT-IR spectra, and HPLC traces) and additional computational data.

References

(1)   Baranoff, E.; Yum, J. H.; Jung, I.; Vulcano, R.; Gratzel, M.; Nazeeruddin, M. K. Cyclometallated Iridium Complexes as Sensitizers for Dye-Sensitized Solar Cells. *Chem. Asian J.* **2010**, *5*, 496-499.

(2)   Bezzubov, S. I.; Kiselev, Y. M.; Churakov, A. V.; Kozyukhin, S. A.; Sadovnikov, A. A.; Grinberg, V. A.; Emets, V. V.; Doljenko, V. D. Iridium(III) 2-Phenylbenzimidazole Complexes: Synthesis, Structure, Optical Properties, and Applications in Dye-Sensitized Solar Cells. *Eur. J. Inorg. Chem.* **2016**, *2016*, 347-354.

(3)   Fleetham, T. B.; Wang, Z.; Li, J. Exploring cyclometalated Ir complexes as donor materials for organic solar cells. *Inorg. Chem.* **2013**, *52*, 7338-7343.

(4)   Gennari, M.; Légalité, F.; Zhang, L.; Pellegrin, Y.; Blart, E.; Fortage, J.; Brown, A. M.; Deronzier, A.; Collomb, M.-N.; Boujtita, M.; Jacquemin, D.; Hammarström, L.; Odobel, F. Long-Lived Charge Separated State in NiO-Based p-Type Dye-Sensitized Solar Cells with Simple Cyclometalated Iridium Complexes. *J. Phys. Chem. Lett.* **2014**, *5*, 2254-2258.

(5)   Huang, J. A.; Yu, J. S.; Guan, Z. Q.; Jiang, Y. D. Improvement in open circuit voltage of organic solar cells by inserting a thin phosphorescent iridium complex layer. *Appl. Phys. Lett.* **2010**, *97*, 143301.

(6)   Mayo, E. I.; Kilsa, K.; Tirrell, T.; Djurovich, P. I.; Tamayo, A.; Thompson, M. E.; Lewis, N. S.; Gray, H. B. Cyclometalated iridium(III)-sensitized titanium dioxide solar cells. *Photochem. Photobiol. Sci.* **2006**, *5*, 871-873.

(7)   Tan, G.; Liu, P.; Wu, H.; Yiu, S.-C.; Dai, F.; Feng, Y.-H.; Liu, X.; Qiu, Y.; Lo, Y. H.; Ho, C.-L.; Wong, W.-Y. New iridium(III) cyclometalates with extended absorption features for bulk heterojunction solar cells. *J. Organomet. Chem.* **2016**, *812*, 280-286.

(8)   Wang, D.; Dong, H.; Wu, Y.; Yu, Y.; Zhou, G.; Li, L.; Wu, Z.; Gao, M.; Wang, G. Effect of diphenylamine substituent on charge-transfer absorption features of the iridium complexes and application in dye-sensitized solar cell. *J. Organomet. Chem.* **2015**, *775*, 55-59.

(9)   Adachi, C.; Baldo, M. A.; Thompson, M. E.; Forrest, S. R. Nearly 100% internal phosphorescence efficiency in an organic light-emitting device. *Journal of Applied Physics* **2001**, *90*, 5048-5051.

(10)   Baldo, M. A.; Thompson, M. E.; Forrest, S. R. High-efficiency fluorescent organic light-emitting devices using a phosphorescent sensitizer. *Nature* **2000**, *403*, 750-753.

(11)   Chiu, Y. C.; Hung, J. Y.; Chi, Y.; Chen, C. C.; Chang, C. H.; Wu, C. C.; Cheng, Y. M.; Yu, Y. C.; Lee, G. H.; Chou, P. T. En Route to High External Quantum Efficiency (similar to 12%), Organic True-Blue-Light-Emitting Diodes Employing Novel Design of Iridium (III) Phosphors. *Advanced Materials* **2009**, *21*, 2221-2225.

(12)   Henwood, A. F.; Bansal, A. K.; Cordes, D. B.; Slawin, A. M. Z.; Samuel, I. D. W.; Zysman-Colman, E. Solubilised bright blue-emitting iridium complexes for solution processed OLEDs. *J. Mater. Chem. C* **2016**, *4*, 3726-3737.

(13)   Ho, C. L.; Wong, W. Y.; Wang, Q.; Ma, D. G.; Wang, L. X.; Lin, Z. Y. A multifunctional iridium-carbazolyl orange phosphor for high-performance two-element WOLED exploiting Exciton-Managed fluorescence/phosphorescence. *Adv. Funct. Mater.* **2008**, *18*, 928-937.

(14)   Jou, J.-H.; Peng, S.-H.; Chiang, C.-I.; Chen, Y.-L.; Lin, Y.-X.; Jou, Y.-C.; Chen, C.-H.; Li, C.-J.; Wang, W.-B.; Shen, S.-M.; Chen, S.-Z.; Wei, M.-K.; Sun, Y.-S.; Hung, H.-W.; Liu, M.-C.; Lin, Y.-P.; Li, J.-Y.; Wang, C.-W. High efficiency yellow organic light-emitting diodes with a solution-processed molecular host-based emissive layer. *J. Mater. Chem. C* **2013**, *1*, 1680-1686.

(15)   Kim, T. H.; Lee, H. K.; Park, O. O.; Chin, B. D.; Lee, S. H.; Kim, J. K. White-light-emitting diodes based on iridium complexes via efficient energy transfer from a conjugated polymer. *Adv. Funct. Mater.* **2006**, *16*, 611-617.

(16)   Lamansky, S.; Djurovich, P. I.; Abdel-Razzaq, F.; Garon, S.; Murphy, D. L.; Thompson, M. E. Cyclometalated Ir complexes in polymer organic light-emitting devices. *J. Appl. Phys.* **2002**, *92*, 1570-1575.

(17)   Li, C. L.; Su, Y. J.; Tao, Y. T.; Chou, P. T.; Chien, C. H.; Cheng, C. C.; Liu, R. S. Yellow and red electrophosphors based on linkage isomers of phenylisoquinolinyliridium complexes:

Distinct differences in photophysical and electroluminescence properties. *Adv. Funct. Mater.* **2005**, *15*, 387-395.

(18)   Lo, S. C.; Namdas, E. B.; Burn, P. L.; Samuel, I. D. W. Synthesis and properties of highly efficient electroluminescent green phosphorescent iridium cored dendrimers. *Macromolecules* **2003**, *36*, 9721-9730.

(19)   Nasr, G.; Guerlin, A.; Dumur, F.; Beouch, L.; Dumas, E.; Clavier, G.; Miomandre, F.; Goubard, F.; Gigmes, D.; Bertin, D.; Wantz, G.; Mayer, C. R. Iridium(iii) soft salts from dinuclear cationic and mononuclear anionic complexes for OLED devices. *Chem. Commun.* **2011**, *47*, 10698-10700.

(20)   Sasabe, H.; Takamatsu, J.-I.; Motoyama, T.; Watanabe, S.; Wagenblast, G.; Langer, N.; Molt, O.; Fuchs, E.; Lennartz, C.; Kido, J. High-efficiency blue and white organic light-emitting devices incorporating a blue iridium carbene complex. *Adv. Mater.* **2010**, *22*, 5003-5007.

(21)   Shavaleev, N. M.; Xie, G.; Varghese, S.; Cordes, D. B.; Slawin, A. M.; Momblona, C.; Orti, E.; Bolink, H. J.; Samuel, I. D.; Zysman-Colman, E. Green Phosphorescence and Electroluminescence of Sulfur Pentafluoride-Functionalized Cationic Iridium(III) Complexes. *Inorg. Chem.* **2015**, *54*, 5907-5914.

(22)   Tokito, S. Recent progress in phosphorescent materials for organic light-emitting devices. *J. Photopolym. Sci. Technol.* **2004**, *17*, 307-313.

(23)   Tsuzuki, T.; Tokito, S. Highly efficient and low-voltage phosphorescent organic light-emitting diodes using an iridium complex as the host material. *Adv. Mater.* **2007**, *19*, 276-280.

(24)   Wang, R. J.; Liu, D.; Zhang, R.; Deng, L. J.; Li, J. Y. Solution-processable iridium complexes for efficient orange-red and white organic light-emitting diodes. *J. Mater. Chem.* **2012**, *22*, 1411-1417.

(25)   Xia, D.; Wang, B.; Chen, B.; Wang, S.; Zhang, B.; Ding, J.; Wang, L.; Jing, X.; Wang, F. Self-host blue-emitting iridium dendrimer with carbazole dendrons: nondoped phosphorescent organic light-emitting diodes. *Angew. Chem.* **2014**, *53*, 1048-1052.

(26)   Bolink, H. J.; Cappelli, L.; Coronado, E.; Parham, A.; Stossel, P. Green light-emitting solid-state electrochemical cell obtained from a homoleptic iridium(III) complex containing ionically charged ligands. *Chem. Mater.* **2006**, *18*, 2778-2780.

(27)   Bolink, H. J.; Coronado, E.; Costa, R. D.; Orti, E.; Sessolo, M.; Graber, S.; Doyle, K.; Neuburger, M.; Housecroft, C. E.; Constable, E. C. Long-Living Light-Emitting Electrochemical Cells - Control through Supramolecular Interactions. *Adv. Mater.* **2008**, *20*, 3910-3913.

(28)   Chen, H. F.; Wu, C.; Kuo, M. C.; Thompson, M. E.; Wong, K. T. Anionic iridium complexes for solid state light-emitting electrochemical cells. *J. Mater. Chem.* **2012**, *22*, 9556-9561.

(29)   Costa, R. D.; Orti, E.; Bolink, H. J. Recent advances in light-emitting electrochemical cells. *Pure Appl. Chem.* **2011**, *83*, 2115-2128.

(30)   Costa, R. D.; Orti, E.; Bolink, H. J.; Graber, S.; Schaffner, S.; Neuburger, M.; Housecroft, C. E.; Constable, E. C. Archetype Cationic Iridium Complexes and Their Use in Solid-State Light-Emitting Electrochemical Cells. *Adv. Funct. Mater.* **2009**, *19*, 3456-3463.

(31)   Evariste, S.; Sandroni, M.; Rees, T. W.; Roldan-Carmona, C.; Gil-Escrig, L.; Bolink, H. J.; Baranoff, E.; Zysman-Colman, E. Fluorine-free blue-green emitters for light-emitting electrochemical cells. *J. Mater. Chem. C* **2014**, *2*, 5793-5804.

(32)   Mydlak, M.; Bizzarri, C.; Hartmann, D.; Sarfert, W.; Schmid, G.; De Cola, L. Positively Charged Iridium(III) Triazole Derivatives as Blue Emitters for Light-Emitting Electrochemical Cells. *Adv. Funct. Mater.* **2010**, *20*, 1812-1820.

(33)   Su, H. C.; Fang, F. C.; Hwu, T. Y.; Hsieh, H. H.; Chen, H. F.; Lee, G. H.; Peng, S. M.; Wong, K. T.; Wu, C. C. Highly efficient orange and green solid-state light-emitting electrochemical cells based on cationic Ir-III complexes with enhanced steric hindrance. *Adv. Funct. Mater.* **2007**, *17*, 1019-1027.

(34)   Zhang, J.; Zhou, L.; Al-Attar, H. A.; Shao, K.; Wang, L.; Zhu, D.; Su, Z.; Bryce, M. R.; Monkman, A. P. Efficient Light-Emitting Electrochemical Cells (LECs) Based on Ionic Iridium(III) Complexes with 1,3,4-Oxadiazole Ligands. *Adv. Funct. Mater.* **2013**, *23*, 4667-4677.

(35)   Mak, C. S. K.; Pentlehner, D.; Stich, M.; Wolfbeis, O. S.; Chan, W. K.; Yersin, H. Exceptional Oxygen Sensing Capabilities and Triplet State Properties of Ir(ppy-NPh2)3. *Chem. Mater.* **2009**, *21*, 2173-2175.

(36)   Marin-Suarez, M.; Curchod, B. F. E.; Tavernelli, I.; Rothlisberger, U.; Scopelliti, R.; Jung, I.; Di Censo, D.; Gratzel, M.; Fernandez-Sanchez, J. F.; Fernandez-Gutierrez, A.; Nazeeruddin, M. K.; Baranoff, E. Nanocomposites Containing Neutral Blue Emitting Cyclometalated Iridium(III) Emitters for Oxygen Sensing. *Chem. Mater.* **2012**, *24*, 2330-2338.

(37)   Xie, Z. G.; Ma, L. Q.; deKrafft, K. E.; Jin, A.; Lin, W. B. Porous Phosphorescent Coordination Polymers for Oxygen Sensing. *J. Am. Chem. Soc.* **2010**, *132*, 922-923.

(38)   You, Y.; Cho, S.; Nam, W. Cyclometalated iridium(III) complexes for phosphorescence sensing of biological metal ions. *Inorg. Chem.* **2014**, *53*, 1804-1815.

(39)   You, Y. M.; Park, S. Y. A Phosphorescent Ir(III) Complex for Selective Fluoride Ion Sensing with a High Signal-to-Noise Ratio. *Adv. Mater.* **2008**, *20*, 3820-3826.

(40)   Liu, J.; Liu, Y.; Liu, Q.; Li, C.; Sun, L.; Li, F. Iridium(III) Complex-Coated Nanosystem for Ratiometric Upconversion Luminescence Bioimaging of Cyanide Anions. *J. Am. Chem. Soc.* **2011**, *133*, 15276-15279.

(41)   Lo, K. K.-W.; Zhang, K. Y. Iridium(iii) complexes as therapeutic and bioimaging reagents for cellular applications. *RSC Adv.* **2012**, *2*, 12069-12083.

(42)   Tang, Y.; Yang, H.-R.; Sun, H.-B.; Liu, S.-J.; Wang, J.-X.; Zhao, Q.; Liu, X.-M.; Xu, W.-J.; Li, S.-B.; Huang, W. Rational Design of an "OFF-ON" Phosphorescent Chemodosimeter Based on an Iridium(III) Complex and Its Application for Time-Resolved Luminescent Detection and Bioimaging of Cysteine and Homocysteine. *Chem. Eur. J.* **2013**, *19*, 1311-1319.

(43)   Zhang, K. Y.; Liu, H. W.; Tang, M. C.; Choi, A. W.; Zhu, N.; Wei, X. G.; Lau, K. C.; Lo, K. K. Dual-Emissive Cyclometalated Iridium(III) Polypyridine Complexes as Ratiometric Biological Probes and Organelle-Selective Bioimaging Reagents. *Inorg. Chem.* **2015**, *54*, 6582-6593.

(44)   Nguyen, J. D.; D'Amato, E. M.; Narayanam, J. M.; Stephenson, C. R. Engaging unactivated alkyl, alkenyl and aryl iodides in visible-light-mediated free radical reactions. *Nat. Chem.* **2012**, *4*, 854-859.

(45)   Nguyen, J. D.; Tucker, J. W.; Konieczynska, M. D.; Stephenson, C. R. J. Intermolecular atom transfer radical addition to olefins mediated by oxidative quenching of photoredox catalysts. *J. Am. Chem. Soc.* **2011**, *133*, 4160-4163.

(46)   Flamigni, L.; Barbieri, A.; Sabatini, C.; Ventura, B.; Barigelletti, F. Photochemistry and photophysics of coordination compounds: Iridium. *Top. Curr. Chem.* **2007**, *281*, 143-203.

(47)   Jiang, J. X.; Yang, W.; Cao, Y. Recent advances in organometallic polymers as highly efficient electrophosphorescent emitters. *J. Inorg. Organomet. Polym. Mater.* **2007**, *17*, 37-55.

(48)   Ulbricht, C.; Beyer, B.; Friebe, C.; Winter, A.; Schubert, U. S. Recent Developments in the Application of Phosphorescent Iridium(III) Complex Systems. *Adv. Mater.* **2009**, *21*, 4418-4441.

(49)   You, Y.; Park, S. Y. Phosphorescent iridium(III) complexes: toward high phosphorescence quantum efficiency through ligand control. *Dalton Trans.* **2009**, 1267-1282.

(50)   Tamayo, A. B.; Alleyne, B. D.; Djurovich, P. I.; Lamansky, S.; Tsyba, I.; Ho, N. N.; Bau, R.; Thompson, M. E. Synthesis and characterization of facial and meridional tris-cyclometalated iridium(III) complexes. *J. Am. Chem. Soc.* **2003**, *125*, 7377-7387.

(51)   Frey, J.; Curchod, B. F. E.; Scopelliti, R.; Tavernelli, I.; Rothlisberger, U.; Nazeeruddin, M. K.; Baranoff, E. Structure-property relationships based on Hammett constants in cyclometalated iridium(III) complexes: their application to the design of a fluorine-free FIrPic-like emitter. *Dalton Trans.* **2014**, *43*, 5667-5679.

(52)   Abe, T.; Miyazawa, A.; Konno, H.; Kawanishi, Y. Deuteration isotope effect on nonradiative transition of fac-tris (2-phenylpyridinato) iridium (III) complexes. *Chem. Phys. Lett.* **2010**, *491*, 199-202.

(53)   Haneder, S.; Da Como, E.; Feldmann, J.; Lupton, J. M.; Lennartz, C.; Erk, P.; Fuchs, E.; Molt, O.; Münster, I.; Schildknecht, C.; Wagenblast, G. Controlling the Radiative Rate of Deep-Blue Electrophosphorescent Organometallic Complexes by Singlet-Triplet Gap Engineering. *Adv. Mater.* **2008**, *20*, 3325-3330.

(54)   Harding, R. E.; Lo, S. C.; Burn, P. L.; Samuel, I. D. W. Non-radiative decay mechanisms in blue phosphorescent iridium(III) complexes. *Org. Electron.* **2008**, *9*, 377-384.

(55)   Karatsu, T.; Ito, E.; Yagai, S.; Kitamura, A. Radiative and nonradiative processes of meridional and facial isomers of heteroleptic irldium-trischelete complexes. *Chem. Phys. Lett.* **2006**, *424*, 353-357.

(56)   Zhou, X.; Burn, P. L.; Powell, B. J. Bond Fission and Non-Radiative Decay in Iridium(III) Complexes. *Inorg. Chem.* **2016**, *55*, 5266-5273.

(57)   Li, J.; Djurovich, P. I.; Alleyne, B. D.; Yousufuddin, M.; Ho, N. N.; Thomas, J. C.; Peters, J. C.; Bau, R.; Thompson, M. E. Synthetic control of excited-state properties in cyclometalated Ir(III) complexes using ancillary ligands. *Inorg. Chem.* **2005**, *44*, 1713-1727.

(58)   Treadway, J. A.; Loeb, B.; Lopez, R.; Anderson, P. A.; Keene, F. R.; Meyer, T. J. Effect of delocalization and rigidity in the acceptor ligand on MLCT excited-state decay. *Inorg. Chem.* **1996**, *35*, 2242-2246.

(59)   Takizawa, S. Y.; Shimada, K.; Sato, Y.; Murata, S. Controlling the excited state and photosensitizing property of a 2-(2-pyridyl)benzo[b]thiophene-based cationic iridium complex through simple chemical modification. *Inorg. Chem.* **2014**, *53*, 2983-2995.

(60)   Baranoff, E.; Curchod, B. F.; Frey, J.; Scopelliti, R.; Kessler, F.; Tavernelli, I.; Rothlisberger, U.; Gratzel, M.; Nazeeruddin, M. K. Acid-induced degradation of phosphorescent dopants for OLEDs and its application to the synthesis of tris-heteroleptic iridium(III) bis-cyclometalated complexes. *Inorganic chemistry* **2012**, *51*, 215-224.

(61)   Edkins, R. M.; Wriglesworth, A.; Fucke, K.; Bettington, S. L.; Beeby, A. The synthesis and photophysics of tris-heteroleptic cyclometalated iridium complexes. *Dalton Trans.* **2011**, *40*, 9672-9678.

(62)   Felici, M.; Contreras-Carballada, P.; Smits, J. M. M.; Nolte, R. J. M.; Williams, R. M.; De Cola, L.; Feiters, M. C. Cationic Heteroleptic Cyclometalated Iridium(III) Complexes Containing Phenyl-Triazole and Triazole-Pyridine Clicked Ligands. *Molecules* **2010**, *15*, 2039-2059.

(63)   Lepeltier, M.; Graff, B.; Lalevee, J.; Wantz, G.; Ibrahim-Ouali, M.; Gigmes, D.; Dumur, F. Heteroleptic iridium (III) complexes with three different ligands: Unusual triplet emitters for light-emitting electrochemical cells. *Org. Electron.* **2016**, *37*, 24-34.

(64)   Liao, J. L.; Chi, Y.; Sie, Z. T.; Ku, C. H.; Chang, C. H.; Fox, M. A.; Low, P. J.; Tseng, M. R.; Lee, G. H. Ir(III)-Based Phosphors with Bipyrazolate Ancillaries; Rational Design,

Photophysics, and Applications in Organic Light-Emitting Diodes. *Inorg. Chem.* **2015**, *54*, 10811-10821.

(65) Park, G. Y.; Kim, Y.; Ha, Y. Iridium complexes containing three different ligands as white OLED dopants. *Mol. Cryst. Liq. Cryst.* **2007**, *462*, 179-188.

(66) Tordera, D.; Delgado, M.; Orti, E.; Bolink, H. J.; Frey, J.; Nazeeruddin, M. K.; Baranoff, E. Stable Green Electroluminescence from an Iridium Tris-Heteroleptic Ionic Complex. *Chem. Mater.* **2012**, *24*, 1896-1903.

(67) Tordera, D.; Serrano-Perez, J. J.; Pertegas, A.; Orti, E.; Bolink, H. J.; Baranoff, E.; Nazeeruddin, M. K.; Frey, J. Correlating the Lifetime and Fluorine Content of Iridium(III) Emitters in Green Light-Emitting Electrochemical Cells. *Chem. Mater.* **2013**, *25*, 3391-3397.

(68) Xu, X.; Yang, X.; Dang, J.; Zhou, G.; Wu, Y.; Li, H.; Wong, W. Y. Trifunctional Ir(III) ppy-type asymmetric phosphorescent emitters with ambipolar features for highly efficient electroluminescent devices. *Chem. Commun.* **2014**, *50*, 2473-2476.

(69) Lepeltier, M.; Dumur, F.; Graff, B.; Xiao, P.; Gigmes, D.; Lalevee, J.; Mayer, C. R. Tris-cyclometalated Iridium(III) Complexes with Three Different Ligands: a New Example with 2-(2,4-Difluorophenyl)pyridine-Based Complex. *Helv. Chim. Acta* **2014**, *97*, 939-956.

(70) Tamura, Y.; Hisamatsu, Y.; Kumar, S.; Itoh, T.; Sato, K.; Kuroda, R.; Aoki, S. Efficient Synthesis of Tris-Heteroleptic Iridium(III) Complexes Based on the Zn2+-Promoted Degradation of Tris-Cyclometalated Iridium(III) Complexes and Their Photophysical Properties. *Inorg. Chem.* **2017**, *56*, 812-833.

(71) Bottcher, H. C.; Graf, M.; Sunkel, K.; Mayer, P.; Kruger, H. [Ir(acac)(eta(2)-C8H14)(2)]: A precursor in the synthesis of cyclometalated iridium(III) complexes. *Inorg. Chim. Acta* **2011**, *365*, 103-107.

(72) Albrecht, M. Cyclometalation Using d-Block Transition Metals: Fundamental Aspects and Recent Trends. *Chem. Rev.* **2010**, *110*, 576-623.

(73) Baranoff, E.; Curchod, B. F. E.; Monti, F.; Steimer, F.; Accorsi, G.; Tavernelli, I.; Rothlisberger, U.; Scopelliti, R.; Grätzel, M.; Nazeeruddin, M. K. Influence of Halogen Atoms on a Homologous Series of Bis-Cyclometalated Iridium(III) Complexes. *Inorg. Chem.* **2012**, *51*, 799-811.

(74) Baranoff, E.; Curchod, B. F. E. FIrpic: archetypal blue phosphorescent emitter for electroluminescence. *Dalton Trans.* **2015**, *44*, 8318-8329.

(75) Park, N. G.; Choi, G. C.; Lee, Y. H.; Kim, Y. S. Theoretical studies on the ground and excited states of blue phosphorescent cyclometalated Ir (III) complexes having ancillary ligand. *Current Applied Physics* **2006**, *6*, 620-626.

(76) Gu, X.; Fei, T.; Zhang, H. Y.; Xu, H.; Yang, B.; Ma, Y. G.; Liu, X. D. Theoretical studies of blue-emitting iridium complexes with different ancillary ligands. *J. Phys. Chem. A* **2008**, *112*, 8387-8393.

(77) Li, H. F.; Winget, P.; Risko, C.; Sears, J. S.; Bredas, J. L. Tuning the electronic and photophysical properties of heteroleptic iridium(III) phosphorescent emitters through ancillary ligand substitution: a theoretical perspective. *PCCP* **2013**, *15*, 6293-6302.

(78) Tsai, H.-R.; Lu, K.-Y.; Lai, S.-H.; Fan, C.-H.; Cheng, C.-H.; Chen, I. C. Metal–Ligand Bonding Strength of Fluoro-Substituted Cyclometalated Iridium(III) Complexes from Raman and Infrared Spectra. *J. Phys. Chem. C* **2011**, *115*, 17163-17174.

(79) Batagoda, B. K. T.; Djurovich, P. I.; Bräse, S.; Thompson, M. E. Synthesis and characterization of phosphorescent cyclometalated Ir and Pt heteroleptic complexes using cyclophane-based chelates. *Polyhedron* **2016**, *116*, 182-188.

(80) Fei, T.; Gu, X.; Zhang, M.; Wang, C.; Hanif, M.; Zhang, H.; Ma, Y. Optical and electronic properties of phosphorescent iridium(III) complexes with phenylpyrazole and ancillary ligands. *Synth. Met.* **2009**, *159*, 113-118.

(81)   Pomarico, E.; Silatani, M.; Messina, F.; Braem, O.; Cannizzo, A.; Barranoff, E.; Klein, J. H.; Lambert, C.; Chergui, M. Dual Luminescence, Interligand Decay, and Nonradiative Electronic Relaxation of Cyclometalated Iridium Complexes in Solution. *J. Phys. Chem. C* **2016**, *120*, 16459-16469.

(82)   Escudero, D.; Thiel, W. Exploring the Triplet Excited State Potential Energy Surfaces of a Cyclometalated Pt(II) Complex: Is There Non-Kasha Emissive Behavior? *Inorg. Chem.* **2014**, *53*, 11015-11019.

(83)   Younker, J. M.; Dobbs, K. D. Correlating Experimental Photophysical Properties of Iridium(III) Complexes to Spin−Orbit Coupled TDDFT Predictions. *J. Phys. Chem. C* **2013**, *117*, 25714-25723.

(84)   You, Y.; Kim, K. S.; Ahn, T. K.; Kim, D.; Park, S. Y. Direct spectroscopic observation of interligand energy transfer in cyclometalated heteroleptic iridium(III) complexes: A strategy for phosphorescence color tuning and white light generation. *J. Phys. Chem. C* **2007**, *111*, 4052-4060.

(85)   You, Y. M.; Park, S. Y. Inter-ligand energy transfer and related emission change in the cyclometalated heteroleptic iridium complex: Facile and efficient color tuning over the whole visible range by the ancillary ligand structure. *J. Am. Chem. Soc.* **2005**, *127*, 12438-12439.

(86)   Vlcek, A. A.; Dodsworth, E. S.; Pietro, W. J.; Lever, A. B. P. Excited-State Redox Potentials of Ruthenium Diimine Complexes - Correlations with Ground-State Redox Potentials and Ligand Parameters. *Inorg. Chem.* **1995**, *34*, 1906-1913.

For Table of Contents Only
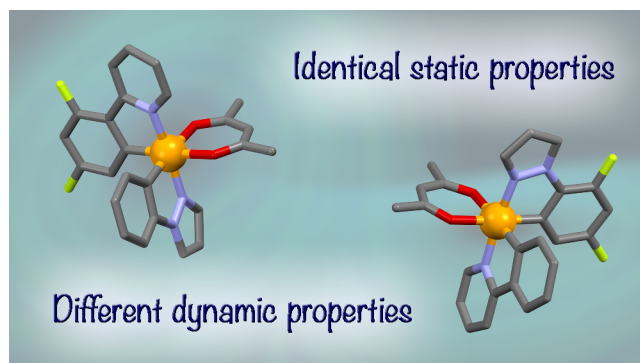
New phosphorescent tris-heteroleptic iridium complexes are reported. The utilization of cyclometalated ligands based on different cores offers an approach for the control of dynamic properties (e.g. excited state lifetime) without impacting static properties (e.g. emission maximum, redox potentials).